DOI: 10.13009/EUCASS2023-007
Aerospace Europe Conference 2023 – 10TH EUCASS – 9TH CEAS

Multi-Objective Multidisciplinary Design Optimization of Regional Truss-Braced Wing Jet Aircraft

Saeed HOSSEINI[†‡], *Mohammad Ali VAZIRY-ZANJANY*[‡], *Hamid Reza OVESY*[‡], *Elyas LEKZIAN*[⋆]
[‡] *Department of Aerospace Engineering, Amirkabir University of Technology, Tehran, Iran.*
[⋆] *Department of Aerospace Engineering, Faculty of New Sciences and Technologies, Semnan University, Semnan, Iran.*
saeed.hosseini@aut.ac.ir · vaziry@aut.ac.ir · ovesy@aut.ac.ir · e.lekzian@semnan.ac.ir
[†]Corresponding author

Abstract

A design optimization methodology is implemented in a multidisciplinary aircraft design framework to optimize a regional very-high aspect ratio truss-braced wing aircraft layout considering both cost and emission requirements. A detailed emission model is incorporated to calculate the emission masses and temperature responses due to the engine emissions. Since the design variables include the mission parameters, namely the cruise altitude and cruise Mach number, an engine sizing module based on the thermodynamic cycle is integrated into the design. The results show that the optimum configuration for emission and cost are quietly different. The emission objective drives the design toward lower cruise altitudes and Mach numbers (i.e. 20 [kft] and Mach 0.4), while the cost objective drives the design toward higher Mach numbers and altitudes. The reason is found to be the mechanism by which these emissions are formed and affect the temperature rise, particularly the altitude at which these emissions are created. At the end, the effect of engine bypass ratio, and mission profile (cruise altitude and cruise speed) are analyzed.

1. Introduction

As air travel demand is estimated to grow by 3.5% annually, the environmental requirements are becoming more and more stringent to mitigate the environmental impacts resulting from increased aircraft emissions. Since the tube-and-wing aircraft configuration has reached a mature state over the decades, the new environmental targets set for the years 2030 and 2050 can be met by the development of novel configurations. These novel configurations not only should provide the capability to increase the performance and reduce the emission significantly, but also it should be economically viable.

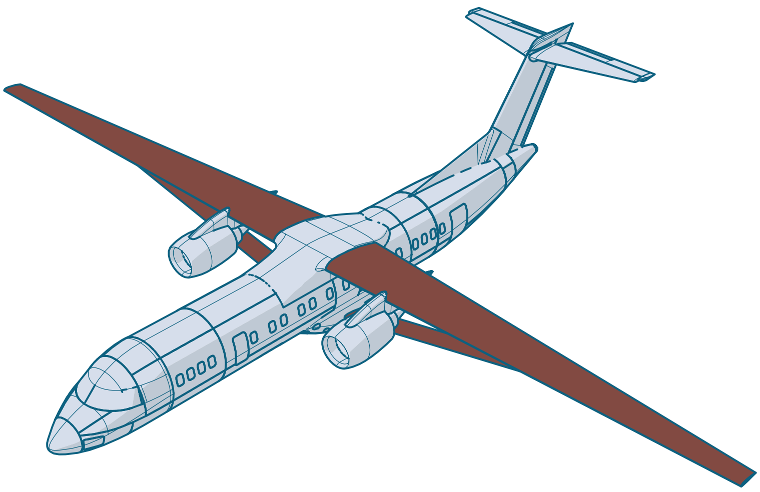

Figure 1: Regional Truss-Braced Wing Aircraft

The very-high aspect ratio truss-braced wing aircraft (Figure 1) is one of the most promising configurations which can reduce fuel burn considerably, and on the other hand, it can incorporate the accumulated know-how, which

DOI: 10.13009/EUCASS2023-007

is the result of decades of tube-and-wing aircraft configuration development. Traditionally, aircraft are designed and optimized for maximum profitability, which has defined the aircraft layout and mission. Considering the emission requirements in the optimization process will result in different layouts and mission profiles, which should be taken into account in the design process.

The emission of a conventional narrow-body aircraft and its effect on the global temperature is formulated in [1], and it was found that the climate-optimum aircraft will have lower cruise altitudes and Mach numbers. Based on this methodology, the effect of fleet planning and engine design parameters were added to the optimization in [2], and the optimum planform and mission characteristics for a narrow-body aircraft were computed. With a different emission methodology, the effect of different technologies on the forward-swept narrow-body aircraft was investigated, and the wing planform was optimized with respect to cost and emissions in [3]. The aircraft emissions at landing and take-off (LTO) were optimized in [4] in conjunction with cost and fuel, and emission-optimum aircraft was found to have a cruise Mach number of 0.41 and an initial cruise altitude of 15 [kft].

In this research, a method for the optimization of the Truss-Braced Wing (TBW) configuration is developed, which takes into account the required number of aircraft based on the market demand, cruise speed, engine on-design conditions, and operational costs. The optimization method is implemented on a regional short-range aircraft, and the effect of design parameters is investigated.

2. Methodology

2.1 Multidisciplinary Framework

A design optimization methodology is developed and implemented in a multidisciplinary aircraft design framework to optimize a regional very-high aspect ratio truss-braced wing aircraft layout considering both cost and emission requirements. This framework is capable of sizing the aircraft, weight analysis, engine analysis, performance analysis, cost analysis, and emission estimation. An aircraft emission analysis module based on existing methodologies is purposely developed for this design framework, which is capable of calculating various types of emission based on the mission profile and aircraft performance. The design framework is presented in Figure 2.

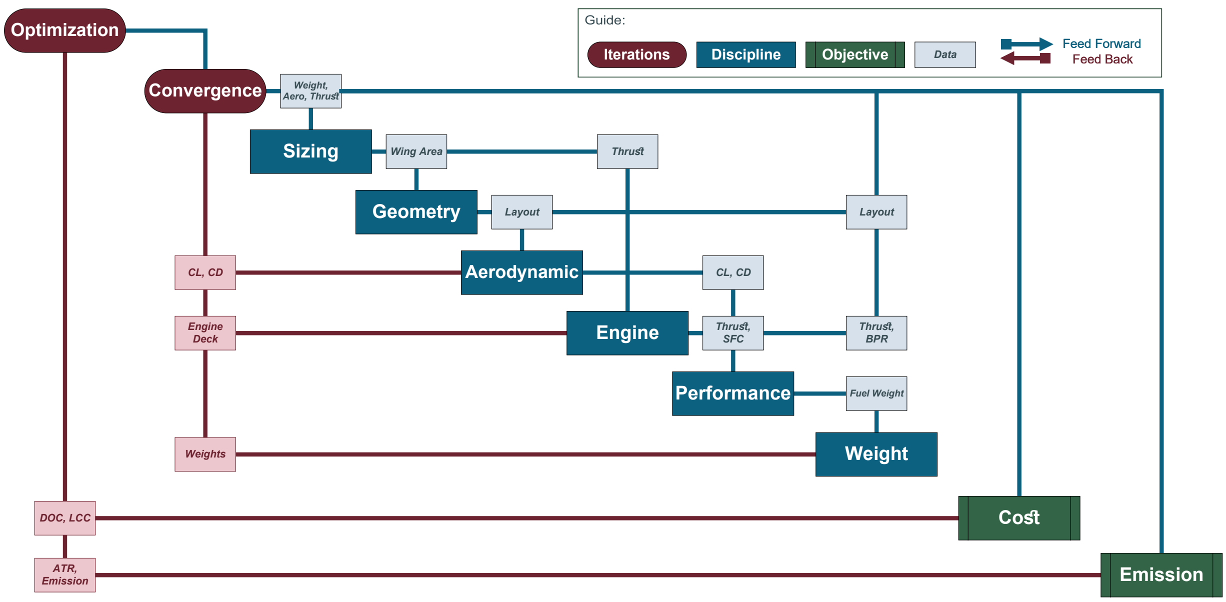

Figure 2: Design and Optimization Framework

The input module parses the input commands and requirements defined by the user, which are stored in a text file. These input commands are validated, are sent for the solution analysis. The design starts with the sizing analysis, in which the wing area and engine thrust are sized based on performance requirements extracted from Part 25 regulations. The computed wing area along with user-defined inputs are then used by the geometrical module, to generate the aircraft layout, including wing, horizontal tail, vertical tail, and fuselage layout. This generated layout is used by the aerodynamic module to compute the aerodynamic characteristics over a wide range of Mach numbers and angle-of-

DOI: 10.13009/EUCASS2023-007

attacks. In the next step, the sized engine thrust is used to generate the engine performance charts (Thrust and TSFC) over the range of Mach numbers and altitudes.

By having the engine performance, aerodynamic characteristics, and aircraft weight, it is possible to calculate the required fuel in the performance module. It should be noted that in the first iteration, where the weight data are not available, an initial value is selected for essential weight parameters. The calculated fuel weight is used to calculate the Maximum Take-Off Weight (MTOW). To this aim, semi-empirical formulas are used to estimate the components and systems' weight based on the mission requirements and geometrical layout. The newly calculated weight and aerodynamic data are passed to the convergence modules, which will be used in the next iteration. This process is repeated by the convergence module until the relative change in take-off weight, wing area, and engine thrust are all below a given threshold, which is selected to be 10^{-5}. The converged aircraft is used to estimate the required number of aircraft for an estimated required seat-kilometer in the next 30 years. The required number of aircraft and aircraft information is used in the cost module to calculate the Direct Operating Cost (DOC), and the Life Cycle Cost (LCC). In the end, the aircraft emission characteristics for the mission and also for its entire life are calculated.

The abovementioned process, which is called Multidisciplinary Design Analysis (MDA) in this research, is included in a higher-level optimization loop, which tries to find optimum design and mission variables. The optimization loop is called Multidisciplinary Design Optimization (MDO).

2.2 Sizing

The required engine thrust and wing area to fulfill the performance requirements, which are based on the mission and Part-25 requirements, are estimated. The static sea-level required engine thrust, T_{SLS}, and the wing area, S_W, are computed using the matching diagram.

Engine Thrust In this research, the requirements of approach, climb's transition segment, the first segment, the second segment, the final segment, AEO go-around, OEI go-around, and take-off distance are considered in the matching diagram.

Wing Area The wing area (S_W) is primarily sized by the desired approach speed and the maximum lift coefficient, C_{Lmax}. The C_{Lmax} is computed from the aerodynamic modules, and is updated in every iteration.

The wing area is related to maximum landing weight (W_L), air density at sea-level (ρ), and the approach speed (V_A) as following:

$$S_W = \frac{W_L}{\frac{1}{2}\rho V_A^2 C_{Lmax}} \tag{1}$$

2.3 Geometry

The design of geometrical components (wing, fuselage, horizontal tail, and vertical tail) layout is carried out using statistical and engineering methods presented in [5]. The design of wing planform parameters is related to the cruise conditions, particularly the Mach number.

2.4 Aerodynamics

The aerodynamic characteristics of the aircraft are computed using a hybrid method combining the Digital DATCOM [6] and the transonic correction.

The drag up to Mach 0.6 is computed using the DATCOM, and Mach numbers above 0.6, the method is extracted from [7]. In this method, the wave drag due to compressibility effects at each Mach number (M) is computed from:

$$C_{Dw} = 20(M - M_{cr})^4 \quad if \quad M > M_{cr} \tag{2}$$

In which, M_{cr} is the critical Mach number. In the original method, the critical Mach number should be computed for each strip of wing section, but in the presented research a single critical Mach number is calculated for the Mean Aerodynamic Chord (MAC). The critical Mach number is computed from Equation 3:

$$M_{cr} = M_{DD} - \left(\frac{0.1}{80}\right)^{\frac{1}{3}} \tag{3}$$

In this equation, M_{DD} is the drag divergence Mach number. The M_{DD} can be computed from [7]:

DOI: 10.13009/EUCASS2023-007

$$M_{DD} \cos \Lambda_{0.5} + \frac{C_L}{10 \cos^2 \Lambda_{0.5}} + \frac{t/c}{\cos \Lambda_{0.5}} = \kappa_A \tag{4}$$

In Equation 4, $\Lambda_{0.5}$ is the sweep angle of mid-chord, C_L is the lift coefficient, t/c is the thickness ratio at MAC, and κ_A is the Korn factor. For supercritical airfoils, $\kappa_A = 0.95$, and for conventional airfoils, $\kappa_A = 0.87$.

Since the nacelle drag and the effect of the BPR are not considered in the DATCOM method, the nacelle drag is added separately to the drag buildup, and the method presented in [8] is used to calculate the drag.

For the TBW configuration, the effects of the strut on the drag are added to the computed drag. It was assumed that the struts provide no lift, and hence will not have any induced drag. The strut friction drag and the wing-strut interference drag are calculated using correction factors, and the associated form factor and interference factor are computed using the method provided in [9]. These factors are based on statistical data and the skin friction coefficient.

2.5 Propulsion

Since the two primary mission parameters, e.g. cruise speed and altitude, are design variables for the optimization, an engine sizing methodology for the required thrust is developed. The thrust of aircraft is provided by two high bypass, separate exhaust, cooled, twin-spool turbofan engines. The Fan and the low-pressure compressor are in balance with the low-pressure turbine through a low-pressure spool. On the other hand, the high-pressure compressor and the high-pressure turbine are connected to the same shaft, referred to as the high-pressure spool. The engine cycle layout is depicted in Figure 3.

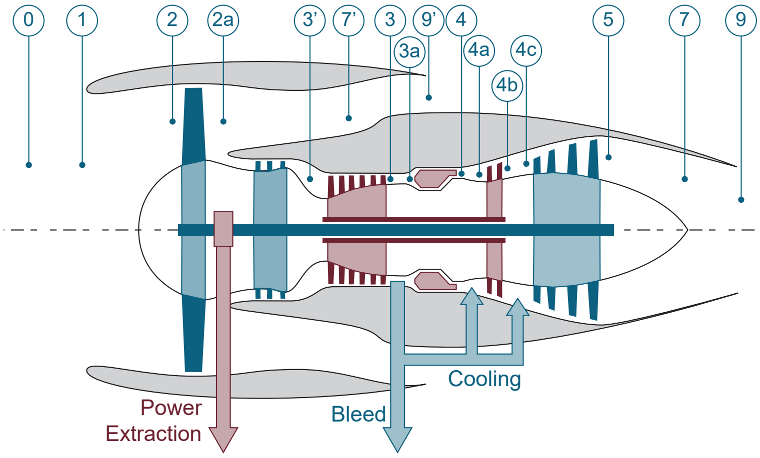

Station	Description
0	Free stream
1	Inlet or diffuser entry
2	Diffuser exit
2a	Fan exit/ Bypass duct entry
3'	Low pressure compressor exit
3	High pressure compressor exit
3a	Burner entry after bleed extraction
4	Burner exit, Nozzle vanes entry
4a	Nozzle vanes exit, Coolant mixer 1 exit
4b	High pressure turbine exit, Nozzle vanes entry
4c	Coolant mixer 2 exit, Low pressure turbine entry
5	Low pressure turbine exit
7	Exhaust nozzle entry
9	Exhaust nozzle exit
7'	Exhaust nozzle entry of bypass duct
9'	Exhaust nozzle exit of bypass duct

Figure 3: Engine Stations for Engine Cycle Design and Analysis

Engine parametric and performance cycle analysis methodology is based on the method presented by Mattingly [10, 11]. Initially, the engine is sized using on-design point data, which is the cruise condition in the current study. Then, the off-design behavior is obtained for all operating conditions utilizing the design point data.

The main design parameters of the engine are the bypass ratio (BPR), overall pressure ratio (OPR), and turbine inlet temperature (TIT). The rest of the required design data, including components' polytropic and isentropic efficiencies, cooling fractions, and power extraction, are considered constant for the on-design and off-design conditions. The pressure losses in the combustion chamber, bypass stream exhaust nozzle, and core stream exhaust nozzle are also constant. The outcome of the performance cycle analysis is the variation of the thrust and thrust specific fuel consumption (TSFC) at different Mach numbers and flight altitudes.

2.6 Weight

The purpose of the weight module is to calculate the buildup of the maximum take-off weight.

Take-Off Weight The maximum take-off weight of the aircraft is expressed as:

$$W_{TO} = W_{OE} + W_{DP} + W_{DF} \tag{5}$$

In which, W_{TO} is the maximum take-off weight, W_{OE} is the operating empty weight, W_{DP} is the design payload weight, and W_{DF} is the design fuel weight.

DOI: 10.13009/EUCASS2023-007

Design Payload Weight Payload weight is calculated from:

$$W_{DP} = n_{pax} \times W_{pax} \tag{6}$$

Where n_{pax} is the number of passengers, and W_{pax} is the weight of the passenger with its baggage. The number of passengers is defined by the input requirements, and 90 $[kg/pax]$ is used for the passenger weight [12].

Operating Empty Weight The operating empty weight is the sum of the manufacturer's empty weight (W_{ME}) and operational items weight (W_{OI}):

$$W_{OE} = W_{ME} + W_{OI} \tag{7}$$

The W_{ME} includes the weight of the structure, powerplant, systems, and interiors. The weight of these items is calculated using a combination of the empirical methods of General Dynamics and Torenbeek method from [13]. Since these systems are similar to conventional designs, except for the wing weight, these methods can be used reliably. For the estimation of wing weight, a calibrated version of the method provided in [14] is employed. The calibration is extracted from high-fidelity finite element analysis and is incorporated into the equation as a constant correction coefficient. For this application, this coefficient has been found to be 0.9. In the engine weight estimation, the effect of bypass ratio is considered using the method provided in [15].

Design Fuel Weight The W_{DF} is the required fuel to fulfill the assigned mission based on the required range and mission profile (cruise altitude and speed). This parameter is calculated in the performance module of the code. This module calculates the performance parameters, including fuel, range, and endurance, for different kinds of phases. The performance analysis considers the variation of thrust, specific fuel consumption, lift, and drag coefficient with Mach number and altitude. The balance of the external acting forces on the aircraft has been taken into account at each time step. Also, this module is capable of finding the cruise phase range based on the required mission range in an iterative process. For further details and validations, interested readers are referred to the mentioned paper [16].

2.7 Cost Analysis

When the MDA loop is converged, the cost analysis is performed to calculate the operating and life-cycle costs.

Life-Cycle Cost The aircraft cost analysis is mainly based on the method presented in [17], and minor modifications are implemented. A short description of the method is presented here, and for more details, readers are referred to the original reference. The aircraft life-cycle cost, the parameter C_{LC}, consists of:

$$C_{LC} = C_{RDTE} + C_{ACQ} + C_{OPS} \tag{8}$$

In which C_{RDTE} is the design, development, and engineering cost, C_{ACQ} is the acquisition cost, and C_{OPS} is the operation cost. The development cost C_{RDTE} includes engineering, tests, prototype aircraft manufacturing, tests, and certification costs. In the development phase, the number of prototypes is assumed to be 4. The engine cost is related to take-off thrust using the statistical formula from [9] (CPI_{2012} is the consumer price index relative to the year 2012):

$$C_{engine} = 1035.9 \times T_{SLS}^{0.8356}\,[lbf] \times CPI_{2012} \tag{9}$$

Fleet Planning One of the parameters that affect costs, particularly the life-cycle cost, is the number of aircraft. Basically, it is common to consider the number of aircraft fixed for the design of aircraft. But, in the real case, the market demand defines the number of aircraft. For example, low-speed flying aircraft may have better performance in terms of fuel consumption and DOC compared to high-speed aircraft. But, on the other hand, high-speed aircraft can carry more passengers, hence it has more productivity. For this reason, to transport the same number of passengers less number of high-speed aircraft and flights are required. To quantify this scenario, it is assumed that this aircraft is designed to provide a fixed number of Available Seat-Kilometers ($ASK(t_0)$) in the first year. This demand is increased annually by $CAGR$ (Compound Annual Growth Rate). The market demand in terms Available Seat-Kilometer (ASK) at year t is calculated from:

$$ASK(t) = ASK(t_0) \times CAGR^{t-t_0} \tag{10}$$

In this research, the analysis is performed for 30 years, i.e. $t_{max} = t_0 + 29$, the initial demand $ASK(t_0)$ is assumed to be 500 $[Billion]$, and the annual growth $CAGR$ is selected as 3%.

DOI: 10.13009/EUCASS2023-007

By knowing the demand each year, the yearly number of required aircraft ($N_{AC}(t)$) and total flights of the fleet ($N_{flight}(t)$) can be computed from:

$$N_{AC}(t) = \frac{ASK(t)\,[km]}{N_{pax} \times U_A\,[h] \times V_B\,[km/h]} \tag{11a}$$

$$N_{flight}(t) = \frac{U_A\,[h]}{E_B\,[h]} \times N_{AC}(t) \tag{11b}$$

In Equation 11, N_{pax} is the number of passengers of the aircraft, U_A is the annual utilization of each aircraft, V_B is the block velocity, and E_B is the block time of the aircraft in the design mission. The U_A is assumed to have a fixed value of 2400 $[h]$, and V_B and E_B are computed from the performance module.

Direct Operating Cost The Direct Operating Cost (DOC), is the sum of operational costs: Flight (fuel cost and crew cost), maintenance, depreciation, fees, and finance costs. The method presented by Roskam in [17] is used for the calculation of DOC.

2.8 Emission Analysis

The emission analysis module calculates the emission of aircraft according to the mission profile, performance, number of flights, and number of aircraft. The primary source of aircraft emissions is the powerplant and engines. Aircraft engines are the sole source of Carbon Dioxide (CO_2) and Nitrogen Oxides (NO_x), and the primary source of noise emissions. In this research, the engine emissions are calculated, but noise is not included in any of the analyses.

Ideal Combustion Process In the combustion of pure fossil fuels (such as Kerosene), only CO_2 and water vapor (H_2O) are generated, see Figure 4.

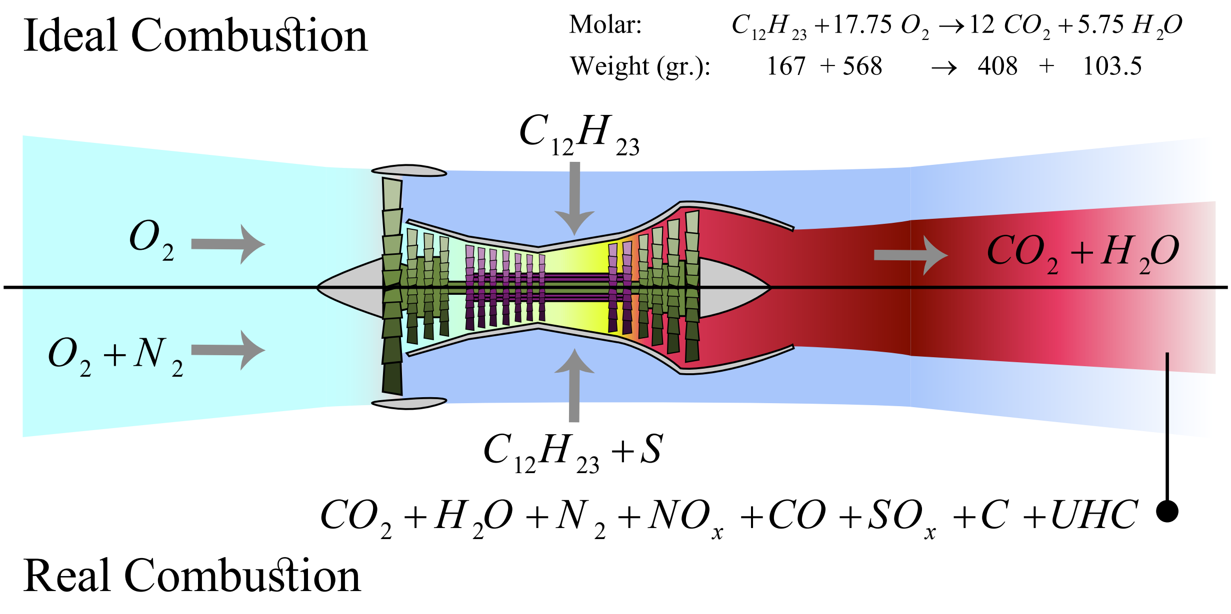

Figure 4: Products of Combustion Process

The combustion formula is as follows:

$$C_{12}H_{23} + 17.75\,O_2 \longrightarrow 12\,CO_2 + 5.75\,H_2O \tag{12}$$

Real Combustion Process But in reality, the combustion process is more complex due to many reasons:

1. Fuels are not pure and contain Sulfur (S) elements. In the combustion process, Sulfur is reacted with Oxygen (O_2), and Sulfur Oxides (SO_x) are produced.
2. Incomplete combustion results in secondary substances, such as Unburned Hydrocarbons (UHC), Carbon Monoxide (CO), and soot.

DOI: 10.13009/EUCASS2023-007

Table 1: Parameters of Emission Species

Species	CO_2	H_2O	NO_x	O_3	CH_4	SO_4	Soot	Contrails
f	1.00	1.14	-	1.37	1.18	0.9	0.7	0.59
EI $[kg/kg]$	3.16	1.26	[1]	-	-	4×10^{-5}	2×10^{-4}	-

3. High temperature combustion oxides the Nitrogen (N_2), which will result in Nitrogen Oxides (NO_x).

It is worth mentioning, that around 0.4% of combustion products are the result of non-ideal combustion. The non-ideal combustion formula, without considering the stoichiometric ratios, is as follows:

$$(C_{12}H_{23} + S) + (O_2 + N_2) \longrightarrow CO_2 + H_2O + N_2 + NO_x + CO + SO_x + \text{Soot} + \text{UHC} \tag{13}$$

Temperature Response In this research it was decided to use the Average Temperature Response (ATR) [18, 19] as a parameter representing the climate impact. This parameter, which has units of temperature (such as mK), shows the increment in the surface temperature of the earth due to pollution of the aircraft over its entire operation. ATR for a period of t_{max} years is calculated from:

$$ATR_{t_{max}} = \frac{1}{t_{max}} \int_{t_0}^{t_{max}} \Delta T(t)dt \tag{14}$$

In Equation 14 the t expressed is in years, t_0 is the first year in the period, and t_{max} is the last year in the period, and $\Delta T(t)$ is the temperature change in each year due emissions produced from the first up to that year. The temperature change is computed from [20]:

$$\Delta T(t) = \int_{t_0}^{t} G(t - t') \times RF^*(t')dt' \tag{15}$$

In Equation 15, RF^* is the normalized radiative forcing (RF), and is equal to one for a doubling in the atmospheric carbon dioxide concentration as compared to preindustrial times, i.e. year 1800.

Radiative Forcing The total normalized radiative forcing is the sum of the normalized radiative forcing of all species:

$$RF^*(t) = \sum_i RF_i^*(t) = \sum_i f_i \frac{RF_i(t)}{RF_{2x \times CO2}} \tag{16}$$

for i= CO_2, H_2O, SO_4, NO_x (CH_4, O_{3L}, O_{3S}), Soot, contrails

Parameter f_i is the efficacy of each element compared to the effects of CO_2, and is equal to the ratio between the climate sensitivity of these species and the climate sensitivity of CO_2. The values for this parameter for many species are presented in Table 1.

Emission Index To calculate the radiative forcing of each pollutant element, the produced mass of that element is required. These masses are calculated using the engine performance and engine characteristics. The engine emission is characterized using the parameter "Emission Index", EI, which is the mass of produced emission per 1 kg of consumed fuel:

$$EI_i = \frac{m_i}{m_F} \tag{17}$$

In this equation, EI_i is the emission index of substance i (such as CO, CO_2, etc.), m_i is the mass of produced emission, and m_F is the mass of consumed fuel. For ideal combustion products, the stoichiometric ratio will be used to calculate the emission index. For non-ideal combustion products, many methods have been developed that can calculate the emission index.

The emissions indices for many combustion products, such as CO_2, H_2O, and SO_x are only related to the engine fuel consumption, and are approximately constant throughout the flight of the aircraft. But, emissions of NO_x, CO, UHC, and soot are highly dependent on many variables, specifically the flight conditions and engine throttle [21]. The emission index for the species is presented in Table 1.

DOI: 10.13009/EUCASS2023-007

Carbon Dioxide CO_2 emissions are the primary pollutant product of the combustion process and have the most significant effect on the atmosphere. The emission mass of carbon dioxide is directly related to the fuel flow, with an approximate emission index of 3.160 $[kg/kg]$ for kerosene fuel. To calculate the radiative forcing of the CO_2 at each year, a method presented in [20] is implemented. In this method, the change concentration of CO_2 at year each year, denoted by $\Delta\chi(t)$, is calculated from:

$$\Delta\chi_{CO2}(t) = \int_{t_0}^{t} G_{\chi_{CO2}}(t - t') \times E_{CO2}(t')dt'$$
$$G_{\chi_{CO2}}(t) = \sum_{i=1}^{5} \alpha_i \times e^{-t/\tau_i} \tag{18}$$

The $E_{CO2}(t)$ in Equation 18 is the emission mass of CO_2 in year t, which is calculated from the emission index. The values for α_i and τ_i are used from [20]. The normalized radiative forcing of the CO_2 is then can be calculated from:

$$RF^{*}_{CO2}(t) = \frac{1}{\ln 2} \ln\left(\frac{\chi_{CO2,0} + \Delta\chi_{CO2}(t)}{\chi_{CO2,0}}\right) \tag{19}$$

The $\chi_{CO2,0}$ in Equation 19 is the background concentration and is equal to equal to 380 ppmv (parts per million volume).

Water Vapour Water (H_2O) vapor is the next primary product of engine combustion, which is a greenhouse gas. Similar to CO_2, the water vapor mass can be calculated from the constant emission index of , 1.260 $[kg/kg]$. The radiative forcing of the water vapor is calculated from:

$$RF_{H2O}(t) = \left(\frac{RF_{ref}}{E_{ref}}\right)_{H2O} E_{H2O}(t) \quad , \quad \left(\frac{RF_{ref}}{E_{ref}}\right)_{H2O} = 7.43 \times 10^{-15} \quad [{}^{W}/_{m^2}/kg] \tag{20}$$

Soot Since the produced Soot has a small contribution, the EI for soot is assumed to be constant, though it can vary with engine operating conditions. The emission index for soot is selected as 2.0×10^{-4} $[kg/kg]$ [22]. The radiative forcing of the soot is calculated from:

$$RF_{Soot}(t) = \left(\frac{RF_{ref}}{E_{ref}}\right)_{Soot} E_{Soot}(t) \quad , \quad \left(\frac{RF_{ref}}{E_{ref}}\right)_{Soot} = 5.0 \times 10^{-10} \quad [{}^{W}/_{m^2}/kg] \tag{21}$$

Sulfur Oxides Due to the high reactivity of Sulfur (S), the presence of Sulfur in aircraft fuel results in Sulfur Oxides (SO_x) in the combustion products. In these emissions, 95% are Sulfur Dioxide (SO_2), and the remaining are Sulfur Trioxide (SO_3). The SO_3 reacts with the water vapor in the exhaust, and forms Sulfuric acid (H_2SO_4). The emission index for SO_4 is selected as 4.0×10^{-5} $[kg/kg]$ [22]. It should be mentioned that the SO_4 has cooling effects, and the radiative forcing has a negative sign. The radiative forcing of the SO_4 is calculated from:

$$RF_{SO4}(t) = \left(\frac{RF_{ref}}{E_{ref}}\right)_{SO4} E_{SO4}(t) \quad , \quad \left(\frac{RF_{ref}}{E_{ref}}\right)_{SO4} = -1.0 \times 10^{-10} \quad [{}^{W}/_{m^2}/kg] \tag{22}$$

Oxides of Nitrogen Oxides of Nitrogen include many gaseous nitrogen oxides, and among them Nitric Oxide (NO) and Nitrogen Dioxide (NO_2) emissions are typically grouped as NO_x. However NO_x are not greenhouse gas, but it has an indirect effect on global warming. NO_x emissions are produced in the combustion chamber, particularly in the highest temperature of it. Since the combustion chamber temperature is dependent on ambient conditions (pressure and temperature) and fuel-air mass ratio. When the equivalence ratio is equal to 1, the NO_x production reaches its maximum. The NO_x emission index is highest at maximum throttle (at take-off), and would be at minimum at idle throttles [21]. For this reason (dependency on ambient conditions and throttle), the emission index calculation of NO_x is not as straightforward as it was for the aforementioned species.

To estimate the emission index of NO_x, many methods are developed. The ICAO engines emission database provides the emission indices at take-off and landing, while the values for the cruise phase are not published. The Boeing's fuel flow method presented in [23], uses the ICAO's engine emission database, to find the emission at the desired conditions. Dallara developed an analytical expression based on combustion chamber conditions (pressure and temperature) [1]. In this research the Dallara method is used:

DOI: 10.13009/EUCASS2023-007

$$EI_{NOx} = 0.0986 \times \left(\frac{p_{T3a}}{101325}\right)^{0.4} - \exp\left(\frac{T_{T3a}}{194.4} - \frac{H_0}{53.2}\right) \tag{23}$$

In which, T_{T3a} and p_{T3a} are the total temperature and pressure before the combustion chamber, and H_0 is the specific humidity. The specific humidity is calculated from [24], and T_{T3a} and p_{T3a} are calculated from the engine cycle (see subsection 2.5).

The NO_x has no direct effect on global warming, but its effect on greenhouse gases should be considered. The NO_x depletes the CH_4 (Methane) and O_{3L} (long-lived Ozone) in the long-term, which has a cooling effect. On the other hand, the NO_x will increases the O_{3S} (short-lived Ozone), which has a warming effect.

Methane The radiative forcing of Methane is computed using:

$$\begin{aligned} RF_{CH4}(t,H) &= s_{CH4}(H) \int_{t_0}^{t} G_{CH4}(t-t') \times E_{NOx}(t')dt' \\ G_{CH4}(t) &= -5.16 \times 10^{-13} \times e^{-t/12} \quad [W/m^2/kg] \end{aligned} \tag{24}$$

The parameter H in Equation 24 is the altitude at which NO_x is generated. Forcing factor $s_{CH4}(H)$ represents the altitude effect and is computed from Figure 5.

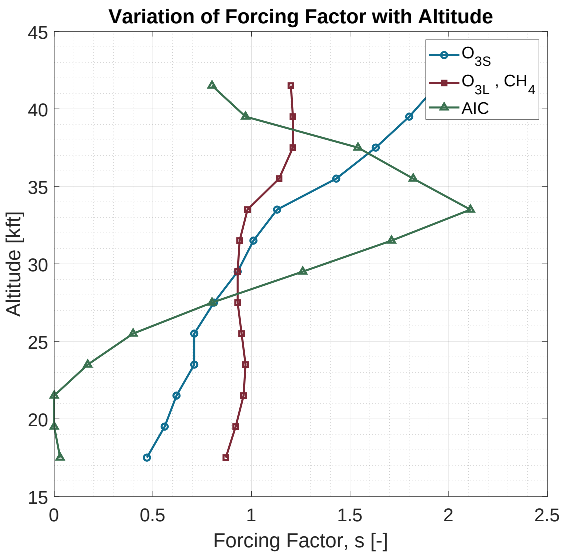

Figure 5: Variation of Forcing Factors with Altitude

Long-Lived Ozone The radiative forcing of O_{3L} is computed using:

$$\begin{aligned} RF_{O3L}(t,H) &= s_{O3L}(H) \int_{t_0}^{t} G_{O3L}(t-t') \times E_{NOx}(t')dt' \\ G_{O3L}(t) &= -1.21 \times 10^{-13} \times e^{-t/12} \quad [W/m^2/kg] \end{aligned} \tag{25}$$

Short-Lived Ozone The radiative forcing of O_{3S} is computed using:

$$RF_{O3S}(t,H) = s_{O3S}(H)\left(\frac{RF_{ref}}{E_{ref}}\right)_{O3S} E_{O3S}(t) \quad , \quad \left(\frac{RF_{ref}}{E_{ref}}\right)_{O3S} = 1.01 \times 10^{-11} \tag{26}$$

Contrails and Aviation-Induced Cloudiness Aviation-Induced Cloudiness (AIC) refers to the combination of contrails and aviation-induced cirrus clouds. The warming effect of AIC is computed from [19]:

$$RF_{AIC}(t) = s_{AIC}(H)\left(\frac{RF_{ref}}{L_{ref}}\right)_{AIC} L_{AIC}(t) \quad , \quad \left(\frac{RF_{ref}}{L_{ref}}\right)_{H2O} = 1.19 \times 10^{-15} \quad [W/m^2/m] \tag{27}$$

In which, L_{AIC} is the total range of all aircraft in a year.

DOI: 10.13009/EUCASS2023-007

2.9 Optimization

Optimization Framework A surrogate optimization methodology based on the Design of Experiment (DoE), Neural Network (NN), and Genetic Algorithm (GA) is implemented to find the results. The overall scheme of this framework is presented in Figure 6.

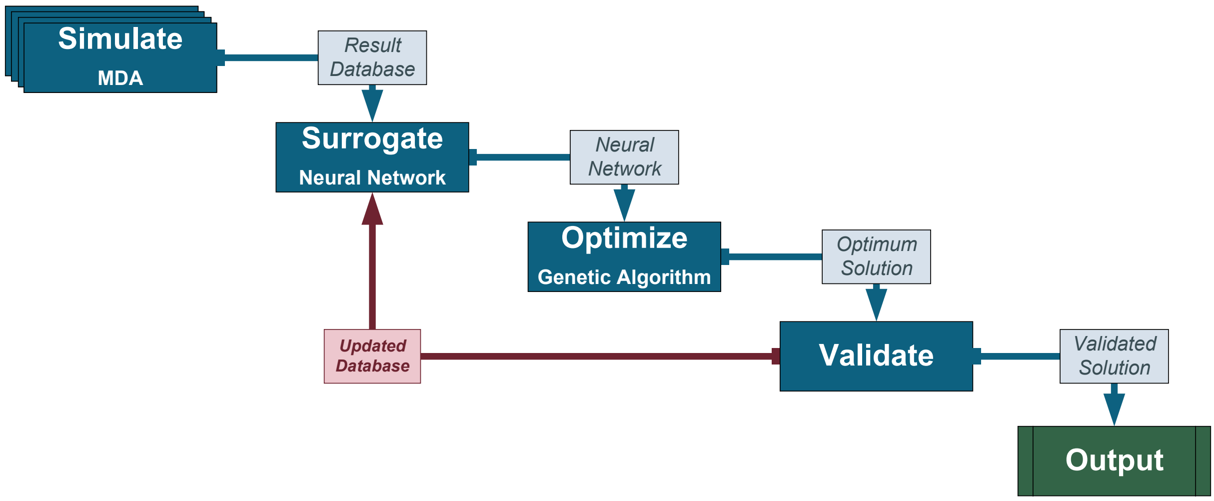

Figure 6: Variation of Forcing Factors with Altitude

Design Variables In the optimization process, the independent design variables are wing span, strut-wing spanwise location, engine bypass ratio, cruise altitude and cruise Mach number. It should be mentioned that there are many other layout parameters, which are dependent variables and are computed based on the independent variables. For example, the wing sweep angle and wing taper ratio are related to the cruise Mach number and wing aspect ratio. The limit and initial value for the design variables are presented in Table 2.

Table 2: Design Variables for MDO

Variable	Lower Limit	Upper Limit	Notes
Wing Tip Y [m]	14.0	24.0	Represents Span and Aspect Ratio
Strut Tip Spanwise [%]	50%	75%	Upper Limit due Stability
Cruise Altitude [kft]	18.0	42.0	
Cruise Mach Number [-]	0.4	0.8	
Engine Bypass Ratio [-]	6.0	16.0	

Design Objectives In this research, cost (both DOC and LCC), weight (MTOW), and emission (ATR) are selected as the objective functions.

Design of Experiments A population of samples is randomly generated using the Latin Hypercube method, and these samples will be used to populate the database. In this research, 200 samples were generated. Each set of design variables is used in the MDA process, and the objective functions are calculated.

Neural Network Neural Network (NN) method is implemented to create and train a surrogate model. This surrogate model is used to guess the objective function based on any set of desired design variables. The network has one hidden layer and 50 neurons.

Genetic Algorithm A Genetic Algorithm (GA) is then used to find the optimum solution by using the developed surrogate NN model. Since the design framework is developed in MATLAB, existing functions and toolboxes from MATLAB are used for NN and GA, and auxiliary functions and codes are added to pass the information to these modules.

DOI: 10.13009/EUCASS2023-007

3. Results

The optimum point for each objective is presented in Table 3. Minimum ATR is achieved at a higher bypass ratio, higher aspect ratio, lower cruise altitude, and lower cruise Mach number. In contrast, lower DOC and LCC are achieved at higher cruise altitudes and cruise Mach numbers. As the cruise speed increases, the wing aspect ratio is reduced, and the optimum points tend to lower the bypass ratio. One of the reasons for a lower bypass ratio at higher speed is that a lower bypass ratio reduces the nacelle drag.

Table 3: Optimum Point

Parameter	ATR	DOC	LCC	MTOW
Wing Tip Y [m]	19.34	17.92	17.11	15.20
Strut Tip Spanwise [%]	69%	70%	73%	67%
Cruise Altitude [kft]	19.95	38.16	37.90	21.34
Cruise Mach Number [-]	0.43	0.65	0.73	0.41
Engine Bypass Ratio [-]	13.95	7.01	6.48	8.58
ATR [mK]	0.309	0.824	0.908	0.333
DOC [USD/pax/trim]	197.8	155.8	156.6	191.6
LCC [BUSD]	3287.4	2559.0	2555.5	3170.0
MTOW [kg]	28,041	26,491	27,989	24,706

The temperature response of the LCC-Optimum and ATR-Optimum designs are presented in Figure 7. As can be seen, flying in higher altitudes, results in considerably higher temperature rise due to aviation-induced cloudiness. Also, as be seen from Figure 5, the AIC and O_3S increase at higher altitudes.

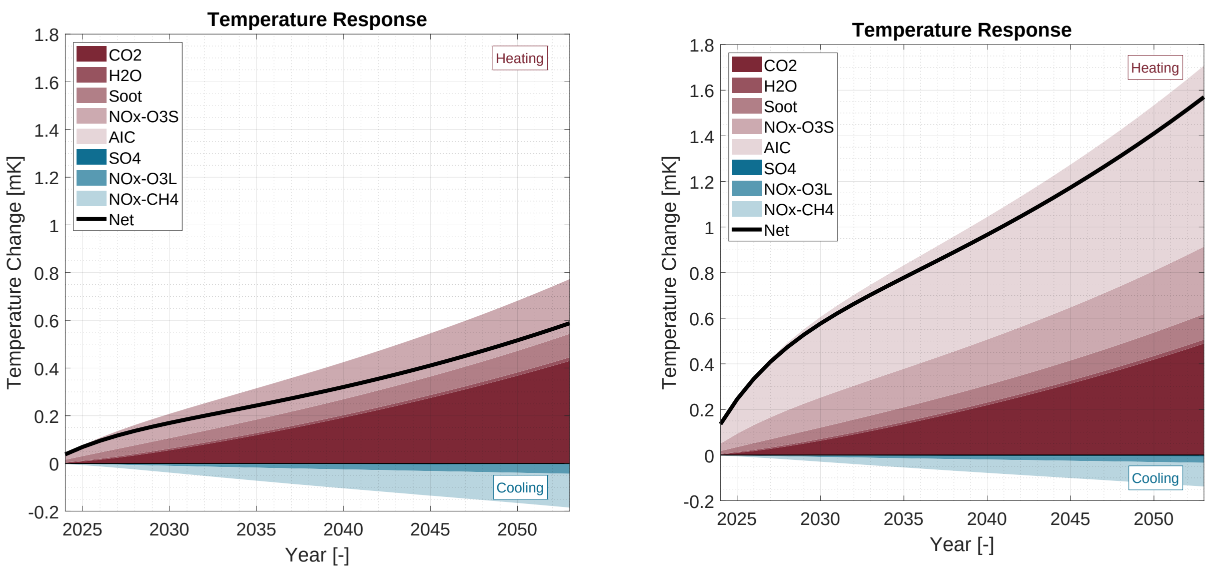

(a) ATR-Optimum

(b) LCC-Optimum

Figure 7: Temperature Rise of Optimum Solutions

The pareto front for LCC, ATR, MTOW, and cruise L/D is presented in Figure 8. As can be seen from Figure 8a, higher cruise altitude, results in higher ATR, while the LCC cost is generally would be lower. The higher speed at higher cruise altitudes can reduce the required number of aircraft, which will reduce the costs. On the other hand, the higher cruise altitude will reduce the AIC warming effects significantly. In contrast, the variation of L/D with MTOW is more dependent on the airframe design, rather than the mission characteristics. As can be seen from Figure 8b and Figure 8c, as the wing aspect ratio increases, the cruise L/D increases accordingly. But, the MTOW initially decreases due reduction in mission fuel, but beyond a point, the wing weight penalty outweighs the fuel reductions and the wing weight increases. The increment in engine BPR results in an increment in both LCC and engine weight, see Figure 8d.

DOI: 10.13009/EUCASS2023-007

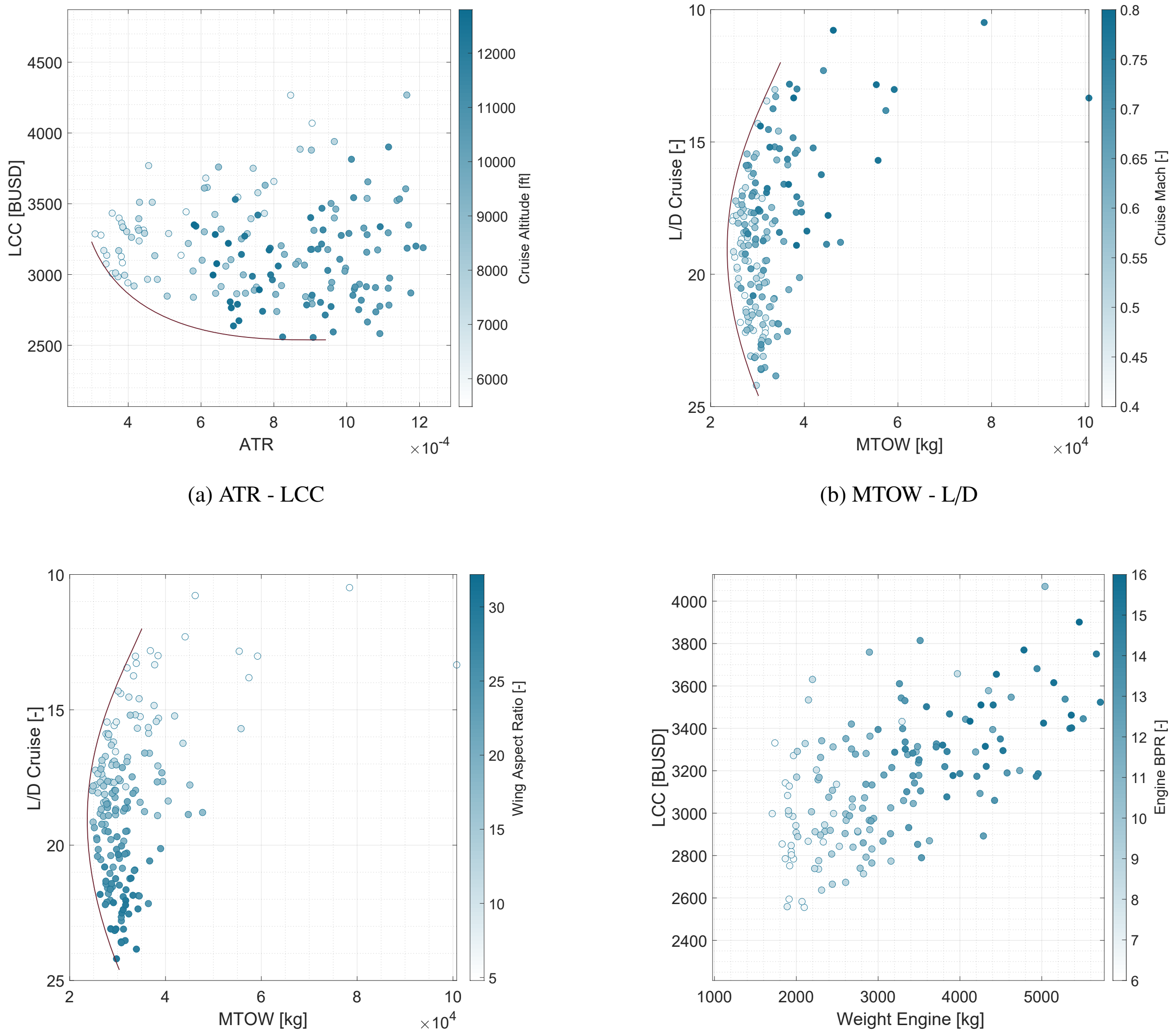

(a) ATR - LCC

(b) MTOW - L/D

(c) MTOW - L/D

(d) Engine Weight - LCC

Figure 8: Pareto Front

4. Conclusion

A methodology for optimizing aircraft mission and wing planform with respect to emission and cost objectives is developed. This methodology is implemented through a multidisciplinary design and optimization framework and is applied to regional truss-braced wing twin-turbofan aircraft. The optimization results show that the cost and emission requirements drive the design toward quite different configurations. The emission requirements, parametrized in average temperature response (ATR), will result in low-flying aircraft, e.g. lower cruise altitudes and lower cruise Mach number. On the other hand, the cost requirements, represented by DOC and LCC, will tend to aircraft with configurations suitable for flying at high altitudes and Mach numbers.

Though it has been tried to capture all possible effects of emission, particularly those that can affect the design at conceptual design, but there are still gaps that require more detailed investigation. The aviation-induced cloudiness model used does not consider the actual environmental conditions at which contrail is formed. In the analysis, it is assumed that the aircraft is flown only in one mission, which is the design mission. But in reality, the majority of flights are done with lower payload and range. A more detailed aerodynamic module may be used to increase the accuracy of the aerodynamic module over the range of Mach numbers. The engine cycle module can be improved to consider the RPM and more details of the thermodynamic cycle.

DOI: 10.13009/EUCASS2023-007

References

[1] Emily Schwartz Dallara. *Aircraft Design for Reduced Climate Impact*. Phd thesis, Department Aeronautics and Astronautics, Stanford University, 2011.

[2] Pieter-Jan Proesmans and Roelof Vos. Airplane design optimization for minimal global warming impact. *Journal of Aircraft*, 59(5):1363–1381, 2022.

[3] Stanislav Karpuk, Rolf Radespiel, and Ali Elham. Assessment of future airframe and propulsion technologies on sustainability of next-generation mid-range aircraft. *Aerospace*, 9(5):279, 2022.

[4] R. P. Henderson, J. R. R. A. Martins, and R. E. Perez. Aircraft conceptual design for optimal environmental performance. *The Aeronautical Journal*, 116(1175):1–22, 2012.

[5] Jan Roskam. *Airplane Design, Part II: Preliminary Configuration Design and Integration of the Propulsion System*. Roskam Aviation and Engineering Corporation, 1985.

[6] R. D. Fink. Usaf stability and control datcom. Report, 1978.

[7] Ohad Gur, William H. Mason, and Joseph A. Schetz. Full-configuration drag estimation. *Journal of Aircraft*, 47(4):1356–1367, 2010.

[8] Jan Roskam. *Airplane Design, Part VI: Preliminary calculation of aerodynamic, thrust and power characteristics*. Roskam Aviation and Engineering Corporation, Kansas, 1987.

[9] Snorri Gudmundsson. *General Aviation Aircraft Design: Applied Methods and Procedures*. Butterworth-Heinemann, 2014.

[10] Jack D Mattingly. *Aircraft Engine Design*. AIAA, 2002.

[11] Jack D Mattingly, Keith M Boyer, and Hans von Ohain. *Elements of Propulsion: Gas Turbines and Rockets*, volume 53. AIAA, 2006.

[12] Jan Roskam. *Airplane Design, Part I: Preliminary Sizing of Aircraft*. Roskam Aviation and Engineering Corporation, Kansas, 1985.

[13] Jan Roskam. *Airplane Design, Part V: Component Weight Estimation*. Roskam Aviation and Engineering Corporation, Kansas, 1985.

[14] Gabriel P. Chiozzotto. Wing weight estimation in conceptual design: a method for strut-braced wings considering static aeroelastic effects. *CEAS Aeronautical Journal*, 7:499–519, 2016.

[15] Lloyd R Jenkinson, Paul Simpkin, and Darren Rhodes. *Civil Jet Aircraft Design*, volume 338. Arnold London, UK, 1999.

[16] Saeed Hosseini, Mohammad Ali Vaziri-Zanjani, and Hamid Reza Ovesy. Conceptual design and analysis of an affordable truss-braced wing regional jet aircraft. *Proceedings of the Institution of Mechanical Engineers, Part G: Journal of Aerospace Engineering*, 2020.

[17] Jan Roskam. *Airplane Design, Part VIII: Airplane Cost Estimation*, volume 8. Roskam Aviation and Engineering Corporation, 1990.

[18] Milind Kandlikar. Indices for comparing greenhouse gas emissions: integrating science and economics. *Energy Economics*, 18(4):265–281, 1996.

[19] Emily Schwartz Dallara, Ilan M. Kroo, and Ian A. Waitz. Metric for comparing lifetime average climate impact of aircraft. *AIAA Journal*, 49(8):1600–1613, 2011.

[20] Robert Sausen and Ulrich Schumann. Estimates of the climate response to aircraft co2 and nox emissions scenarios. *Climatic Change*, 44(1/2):27–58, 2000.

[21] Emily S. Nelson and Dhanireddy R. Reddy. *Green Aviation: Reduction of Environmental Impact Through Aircraft Technology and Alternative Fuels*. CRC Press, 2017.

DOI: 10.13009/EUCASS2023-007

[22] Joyce E Penner, David Lister, David J Griggs, David J Dokken, and Mack McFarland. *Aviation and the global atmosphere: a special report of the Intergovernmental Panel on Climate Change*. Cambridge University Press, 1999.

[23] Doug DuBois and Gerald C. Paynter. “fuel flow method2” for estimating aircraft emissions. In *SAE Technical Paper Series*. SAE, 2006.

[24] ISO. ISO 5878: Reference atmospheres for aerospace use, 1982.